ANTIOXIDANTS & REDOX SIGNALING
Volume 15, Number 5, 2011
© Mary Ann Liebert, Inc.
DOI: 10.1089/ars.2011.3895

Amyloid Beta Induces Oxidative Stress-Mediated Blood–Brain Barrier Changes in Capillary Amyloid Angiopathy

Anna Carrano, Jeroen J.M. Hoozemans, Saskia M. van der Vies, Annemieke J.M. Rozemuller, Jack van Horssen*, and Helga E. de Vries*

Abstract

Cerebral amyloid angiopathy (CAA) is frequently observed in Alzheimer's disease (AD) and is characterized by deposition of amyloid beta (Aβ) in leptomeningeal and cortical brain vasculature. In 40% of AD cases, Aβ mainly accumulates in cortical capillaries, a phenomenon referred to as capillary CAA (capCAA). The aim of this study was to investigate blood–brain barrier (BBB) alterations in CAA-affected capillaries with the emphasis on tight junction (TJ) changes. First, capCAA brain tissue was analyzed for the distribution of TJs. Here, we show for the first time a dramatic loss of occludin, claudin-5, and ZO-1 in Aβ-laden capillaries surrounded by NADPH oxidase-2 (NOX-2)-positive activated microglia. Importantly, we observed abundant vascular expression of the Aβ transporter receptor for advanced glycation endproducts (RAGE). To unravel the underlying mechanism, a human brain endothelial cell line was stimulated with Aβ1-42 to analyze the effects of Aβ. We observed a dose-dependent cytotoxicity and increased ROS generation, which interestingly was reversed by administration of exogenous antioxidants, NOX-2 inhibitors, and by blocking RAGE. Taken together, our data evidently show that Aβ is toxic to brain endothelial cells via binding to RAGE and induction of ROS production, which ultimately leads to disruption of TJs and loss of BBB integrity. *Antioxid. Redox Signal.* 15, 1167–1178.

Introduction

Alzheimer's disease (AD) is the most common neurological disorder affecting elderly and is clinically characterized by a progressive cognitive decline associated with extracellular accumulation of neurotoxic amyloid β (Aβ) and hyperphosphorylated tau-positive neurofibrillary tangles (10, 20). Senile plaques predominantly consist of Aβ deposits and can be observed throughout the cerebral cortex in advanced stages of the disease. Alternatively, Aβ is able to accumulate in the cerebrovasculature, which is referred to as cerebral amyloid angiopathy (CAA). CAA is a common finding in the elderly, with an incidence up to 50% of the population (31). There is a strong association between AD and CAA as CAA occurs in 80%–100% of AD cases. CAA can be widespread and is usually observed in larger vessels, including leptomeningeal vessels and cortical arteries and arterioles. Remarkably, Aβ depositions are also observed in cortical capillaries (2). Several groups support the distinction between CAA present in larger vessels (CAA type II) and Aβ accumulation in both larger vessels and capillaries (CAA type I or capillary CAA (capCAA) (37). CAA is a major cause of hemorrhagic and ischemic strokes in elderly patients, probably also involved in microbleeds (3, 39), and may play a role in AD progression. Relatively little is known on the impact of capCAA in AD pathogenesis, although it is tempting to speculate that Aβ accumulation in capillaries may affect blood–brain barrier (BBB) integrity. Notably, BBB dysfunction has been reported in various neurological conditions, including multiple sclerosis, cerebral ischemia, and AD (9, 16, 49, 50).

The BBB is a tight sealed barrier between the circulating blood and the central nervous system (CNS), consisting of brain microvascular endothelial cells that are surrounded by basement membranes, astrocytic endfeet, and pericytes. The brain microvascular endothelium is characterized by the presence of tight junctions (TJs) and lack of fenestrae, thereby limiting the entry of plasma components, red blood cells, and leukocytes into the CNS, and confer the low paracellular permeability and high electrical resistance of the BBB (16, 50). TJs are complex structures located at the apical region between endothelial cells and are composed of connecting

Departments of Molecular Cell Biology and Immunology (MCBI) and Pathology, VU University Medical Center, Amsterdam, The Netherlands.
*These authors contributed equally to this work.

transmembrane proteins (occludin and claudins) that form the primary seal linked via accessory cytoplasmic proteins (zona occludens family members) to the actin cytoskeleton (16).

Occludin is a phosphoprotein with four transmembrane domains and intracellular amino and the carboxyl termini (6a). Occludin expression is associated with increased electrical resistance and decreased paracellular transport. Claudins comprise a multigene family consisting of more than 20 members and contain two extracellular loops and four transmembrane domains and interact in both a homophilic and heterophilic way with claudins of adjacent cells. Claudin-5 is a critical component of the BBB as it prevents the passage of molecules larger than 800 Da (28). Carboxyterminal parts of both occludin and claudins interact with membrane-associated recruiting proteins of the zona occludens (ZO) protein family. ZO proteins are reported to link transmembrane proteins to the actin cytoskeleton and have signaling potential (14).

Leakage of the BBB in AD has been suggested by the detection of plasma proteins associated with amyloid plaques (1, 21, 45) and within AD brain parenchyma (21, 45, 49). Likewise, in CAA, an impaired barrier function was detected associated with cerebrovascular Aβ deposits (45). Opening of the BBB and concomitant altered TJ expression or localization has been attributed to vascular Aβ aggregates (6, 15, 27, 36), which in turn are able to induce reactive oxygen species (ROS) production, mainly generated by NADPH oxidase (NOX), in neuronal and non-neuronal cell cultures (4, 23, 47). Both endogenous and exogenous ROS induce loss of endothelial cell–cell interactions (40) and are able to modulate BBB integrity and disrupt TJs (22, 34). However, to date, the link between Aβ, ROS production and TJs alterations remains elusive.

The involvement of RAGE appears to be very important in the development of the AD and CAA pathology, since RAGE mediates the influx of Aβ into the brain parenchyma and consequently in an unbalanced situation enhances Aβ accumulation. RAGE is also known to be critical regarding the effects exerted by Aβ through its binding to the transporter. Aβ/RAGE interaction has been reported to activate NOX and a cascade of effects such as NF-kB-mediated endothelial activation resulting in secretion of proinflammatory cytokines, the expression of adhesion molecules and suppression of cerebral blood flow (50).

In this study, we combine neuropathological findings in unique brain samples of capCAA patients and show a dramatic loss of TJ proteins in Aβ-laden capillaries. Interestingly, capCAA-affected vessels are surrounded by NOX2-immunopositive activated microglia. We next investigated the link between Aβ toxicity and TJ changes using a human cerebral microvascular endothelial cell line and demonstrated that cytotoxic Aβ via production of ROS, decreased TJ proteins expression which could be rescued by exogenous antioxidants, NOX-2 inhibition, and RAGE blocking antibody.

Materials and Methods

Postmortem tissue

Six patients with extensive capCAA and two age-matched non-demented controls were selected. Human brain specimens were obtained at autopsy with a short postmortem interval (The Netherlands Brain Bank, Amsterdam, The Netherlands and University Medical Centre in Utrecht, The Netherlands). Neuropathological evaluation was performed on frozen tissue and formalin-fixed, paraffin-embedded tissue from occipital pole cortex. CapCAA score was defined as follow: severe (+++), moderate (++), and mild (+). Staging of AD was evaluated according to Braak and colleagues (7). Age, gender, postmortem delay (PMD), Braak, CERAD, and CAA scores and cause of death of all cases used in this study are listed in Table 1.

Immunohistochemistry

For immunohistochemical staining, 5-μm cryosections were air-dried and fixed in acetone for 10 min. Next, sections were preincubated with normal goat serum 1:10, diluted in phosphate buffered saline (PBS) containing 1% bovine serum albumin (Roche Diagnostics, Mannheim, Germany) for 10 min. Sections were incubated O/N with primary antibodies: anti-occludin (mouse, Zymed), anti-ZO1 (rabbit, Zymed) (Table 2) diluted in PBS containing 1% bovine serum albumin. Subsequently, sections were incubated with EnVision goat-anti-mouse horseradish peroxidase (HRP) or EnVision goat-anti-rabbit HRP (Dako, Glostrup, Denmark) for 60 min. Peroxidase labeling was visualized by EnVision 3,3-diaminobenzidine 1:50 (EV-DAB; Dako). Sections were counterstained with hematoxylin. Finally, tissue sections were rinsed with 70% ethanol prior to a 20 min incubation with 50 ml saturated NaCl solution (0.5 *M* NaCl in 80% ethanol) which was supplemented with 0.5 ml 1% NaOH solution. Then sections were transferred to saturated Congo Red (VWR internationaal, Leuven, the Netherlands) solution supplemented with 0.5 ml 1% NaOH solution for 20 min. Congo Red staining was used to visualize Aβ fibrils. Between all incubation steps, sections were extensively washed with PBS (pH 7.4). PBS served as negative control.

Paraffin sections (5 μm) were mounted on coated glass slides (Menzel Gläzer super frost PLUS, Brainschweig, Germany) and dried O/N at 37°C. Sections were deparaffinized

Table 1. Summary of Patient Details

Patient #	*Age*	*Gender*	*PMD*	*Braak*	*CERAD*	*CAA*	*Cause of death*
1	75	F	6	V	0	+++	Dehydration
2	65	M	7	V	C	++/+++	Pneumonia
3	83	F	5	III	B	++/+++	cachexia by dementia syndrome
4	71	F	<24	IV	B	+++	Pneumonia
5	86	M	>24	VI	B	+	Pneumonia
6	78	F	–	IV	A	+++	Pneumonia

Table 2. Primary Antibodies Used in this Study

Primary Antibody	*Species raised in*	*Dilution*	*Method*	*ARS*	*Source*
Occludin	mouse	1:200	EnVision	EDTA	Zymed (Invitrogen)
Claudin-5	mouse	1:200	EnVision	Na-citrate	Zymed (Invitrogen)
ZO-1	rabbit	1:100	ABC	–	Zymed (Invitrogen)
NOX-2	mouse	1:100	EnVision	Na-citrate	Gift of D. Roos
RAGE	goat	1:500	ABC	–	Biochem
Factor VIII	rabbit	1:250	ABC	–	DAKO
CD31	mouse	1:10	ABC	–	DAKO

and rehydrated by xylene and a sloping concentration of ethanol (100%, 96%, and 70%). Endogenous peroxidase was blocked by incubating the sections in methanol + 0.3% H_2O_2 for 30 min. Antigen retrieval was established by boiling the sections in 1 m*M* EDTA buffer for 10 min. Then, sections were O/N incubated with anti-claudin-5 (mouse, Zymed) or anti-NOX2 (mouse) (see Table2) diluted in PBS supplemented with 1% BSA. Then the sections were incubated for 30 min with EnVision anti-rabbit/anti-mouse HRP. Peroxidase labeling was visualized by EVDAB 1:50. Sections were counterstained with hematoxylin. The sections were stained with Congo Red as described above. Finally sections were rinsed twice with 100% ethanol, put in xylene and covered with DePeX mounting medium (Gurr, Germany). Between all incubation steps, sections were extensively washed with PBS (pH 7.4). PBS served as negative control.

Immunofluorescence

For co-localization studies, cryosections were incubated in thioflavin S solution (100 mg/ml) for 5 min to stain Aβ fibrils and washed subsequently three times in ethanol 70%. Sections were preincubated with normal goat serum 1:10 for 10 min and incubated O/N with a mix of primary antibodies: anti occludin/claudin-5 and anti factor VIII or anti ZO-1/RAGE and anti CD31 diluted in PBS containing 1% bovine serum albumin. Sections were then incubated with secondary antibodies: Cy5 labeled goat-anti-rabbit 1:100, diluted in EnVision goat-anti-mouse HRP (Dako) for 30 min. Peroxidase labeling was visualized by reaction with rhodamine-tyramide (1:3000) in presence of 0.01% of H_2O_2 for 5 min. After washing, slides were covered with Vectashield (Vector laboratories, Burlington, ON, Canada). Between all incubation steps, sections were extensively washed with PBS (pH 7.4). Fluorescent analysis was performed with a Leica TCS SP2 AOBS confocal laser-scanning microscope (Leica Microsystem, Heidelberg, Germany). Quantification of TJ protein-expressing vessel was also performed normal vessels versus Aβ-laden vessels. Four fields per slides were counted and a ratio was calculated (magnification X10).

Cell culture

A human cerebral microvascular endothelial cell line (hCMEC/D3) (44) was maintained in EBM-2 medium (Clonetics, Cambrex BioScience, Wokingham, UK) supplemented with VEGF, IGF-1, EGF, basic FGF, hydrocortisone, ascorbate, gentamycin, and 2.5% fetal bovine serum (FBS) 40. T75 flasks, 96-well plates and 24-well plates were coated with type 1 collagen (Gibco HBSS, Invitrogen, Carlsbad, CA). hCMECs were detached at 37°C with 2 ml trypsin/EDTA in PBS. Cultures were grown to confluence at 37°C in 5% CO_2 until the formation of monolayers.

Aβ1-42 preincubation

Synthetic Aβ1-42 (Bachem, Bubendorf, Switzerland) was dissolved in 0.1% ammonium hydroxide and stored in 50 μl, 1 m*M* aliquots at −80°C. 40 μM Aβ1-42 was preincubated in EBM-2 medium without FBS for 3 days in order to form aggregates. Then Aβ1-42 was further diluted in cell medium to obtain appropriate concentrations.

Electron microscopy

Pre-aggregated Aβ1-42 was applied to formvar carbon-coated copper grids (Stork Veco BV, Eerbeek, The Netherlands) and dried for 10 min. Grids were negatively stained with uranyl acetate for 5 min and examined with a Zeiss EM109 electron microscope to visualize the formation of fibrils.

MTT assay

The cytotoxicity of synthetic Aβ1-42 preparations was assessed by the 3-(4,5-dimethylthiazol-2-yl)-2,5-diphenyltetrazolium bromide (MTT; Sigma Aldrich, Germany) assay. hCMECs were cultured in 96-well plates until they reached 100% confluence. Cells were incubated for 24 h with different concentrations of Aβ1-42 (1 n*M*, 10 n*M*, 100 n*M*, 1 μM, 10 μM). Antioxidants and blocking antibody anti-RAGE were applied 2 h prior Aβ incubation and were still present during the entire treatment. Then cells were incubated with MTT (1 mg/ml) for 3 h at 37°C. The formazan-salt generated by mitochondria of viable cells as a result of conversion of MTT was dissolved in glycin/DMSO (ratio 1:6) and the absorbance was measured at 540 nm.

Live/dead assay

Using the LIVE/DEAD Viability/Cytotoxicity Assay Kit (Molecular Probes Inc, Eugene, OR) living and dead cells can be distinguished from each other. hCMECs were cultured in 96-well plates until they reached 100% confluence. Cells were incubated for 24 h with different concentrations of Aβ1-42 (1 μM, 10 μM, 20 μM). Cells were washed gently with warm PBS. Then 1 μl calcein AM and 1.5 μl ethidium homodimer 1 were added to warm EBM-2 medium and 100 μl of this mixture was added per well for 20 minutes. The cell permeable calcein AM is converted into the green fluorescent calcein by intracellular esterase activity (excitation ~495 nm; emission ~515 nm).

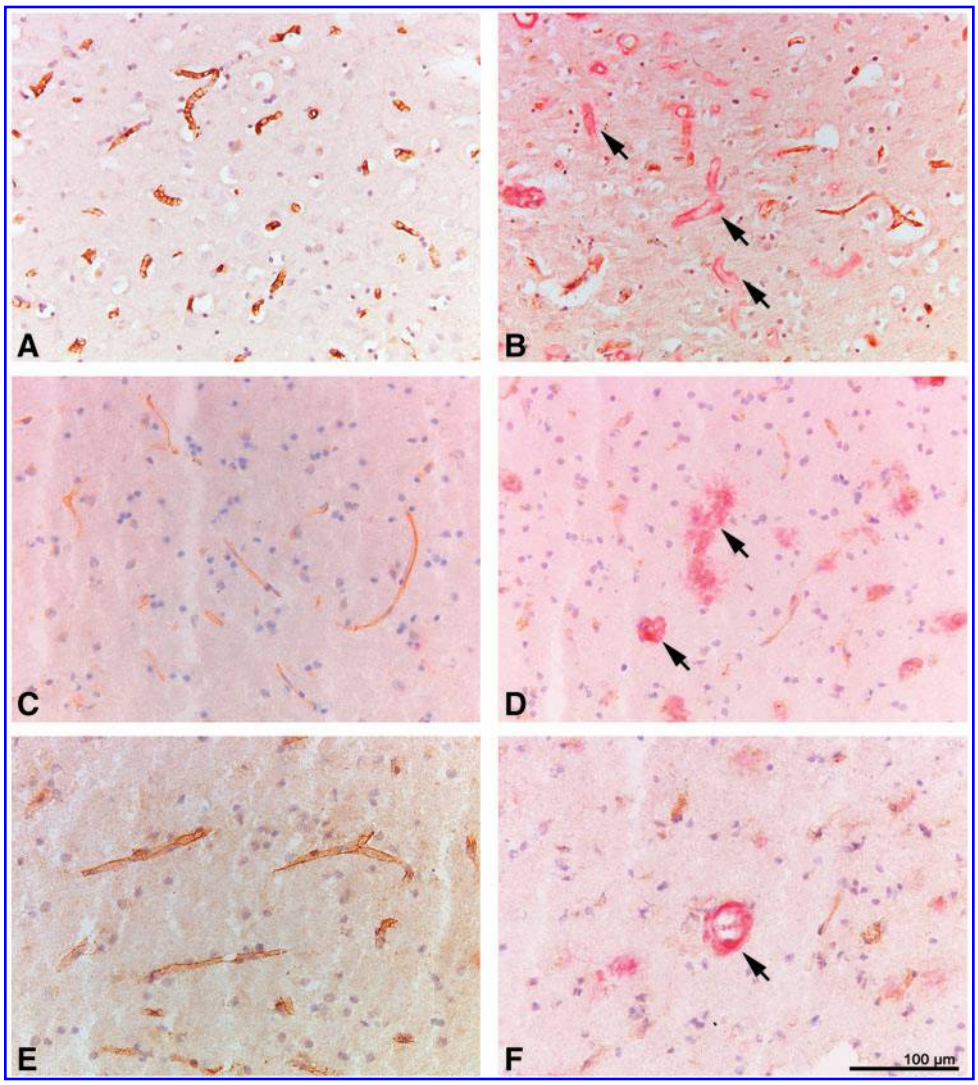

FIG. 1. Loss of TJ proteins in capCAA. TJ proteins (*brown*) are normally expressed in endothelial cells of capillaries. Claudin-5 immunoreactivity was localized virtually in all the vasculature in control and unaffected tissue **(A)**. Loss of endothelial claudin-5 was observed in Aβ-laden capillaries (Congo red) (*arrows*) **(B)**. Occludin immunoreactivity was localized virtually in all the vasculature in control and unaffected tissue **(C)**. Loss of occludin in endothelial cells was observed in Aβ-laden capillaries indicated by the *arrows* **(D)**. ZO1 expression was detected in the vasculature of control and unaffected tissue **(E)**. Loss of ZO1 in endothelial cells was observed in Aβ-laden capillaries indicated by the *arrow* **(F).** (To see this illustration in color the reader is referred to the web version of this article at www.liebertonline.com/ars).

Ethidium homodimer 1 is able to enter cells with damaged membranes. It undergoes a 40-fold enhancement of fluorescence upon binding to nucleic acids and produces a red fluorescent signal in dead cells (excitation ~495 nm, emission ~635nm). Four 10 times magnified fields were counted and a ratio was calculated for live and dead cells.

Amplex Red assay

hCMECs were cultured in 96-well plates until they reached 100% confluence. Cells were treated with different concentrations of Aβ1-42 (1 n*M*, 10 n*M*, 100 n*M*, 1 μ*M*, and 10 μ*M*) for 24 h. After incubation, Aβ was removed and H_2O_2 production was detected using the Amplex red fluorescent dye (Molecular Probes, Breda, the Netherlands) which reacts 1:1 with H_2O_2 in the presence of horseradish peroxidase, producing highly fluorescent resorufin. Fluorescence was detected at 37°C in a fluorimeter (Galaxy-Fluostar, BMG, Offenburg, Germany). The excitation and emission fluorescent wavelengths were 550 and 590 nm, respectively. The calibration signal was produced by addition of known amounts of H_2O_2 added to the reaction mix. The velocity whereby H_2O_2 was produced was calculated using non-linear regression.

mRNA isolation and real-time quantitative PCR

To investigate mRNA expression of TJ proteins cells were grown on a 24-well plate until they reached 100% confluency. Cells were incubated with different concentrations of Aβ1-42 (10 n*M*, 100 n*M*, 1 μ*M*) for 24 h. mRNA was isolated by using the mRNA capture kit (Roche Applied Science, Almere, the Netherlands) following the manufacturer's protocol. mRNA was reverse transcribed using the Reverse transcription system kit (Promega, Madison, WI) according to the manufacturer's instructions using GeneAmp PCR system 9700 (Applied Biosystems, Foster City, CA). cDNA was diluted three times and quantified for mRNA levels of occludin/claudin-5/ZO-1 relative to the housekeeping gene GAPDH. The accumulation of PCR product is measured using Sybergreen II (Applied Biosystems). Primers were developed using the program Primer Express 2.0 (Applied Biosystems). The sequences of primers are as follows: human occludin: sense 5′-CCCGTTTGGATAAAGAATTGG-3′, antisense 5′-TCAAAC AACTTGGCATCAGA-3′; human ZO-1: sense 5′-CCCGAAG GAGTTGAGCAGGAAATC-3′, antisense 5′-CCACAGGCT TCAGGAACTTGAGG-3′. The PCR amplification was performed in triplicate in a 7900 HT Fast Real-Time PCRSystem

(Applied Biosystems). Relative expression levels of TJ proteins in relation to the reference GAPDH were calculated using the mathematical model: ΔΔCT. The formula is 2-ΔΔCT where ΔCT = CTtarget - CTreference and ΔΔCT = ΔCTsample - ΔCTcalibrator.

Statistical analysis

Data were analyzed statistically by Student's *t*-test or analysis of variance (ANOVA) followed by post hoc analysis with Bonferroni's method (*$P < 0.05$, **$P < 0.01$, ***$P < 0.001$).

Results

Reduced tight junction protein expression in CapCAA-affected vessels

Using Congo Red, we observed extensive Aβ deposits throughout the occipital cortex in capillaries and larger vessels. No Aβ was detected in brain vessels of control brains. To investigate the expression of TJ proteins, postmortem tissue of 6 capCAA patients and 2 non-neurological controls was stained for occludin, claudin-5, and ZO-1. We observed a

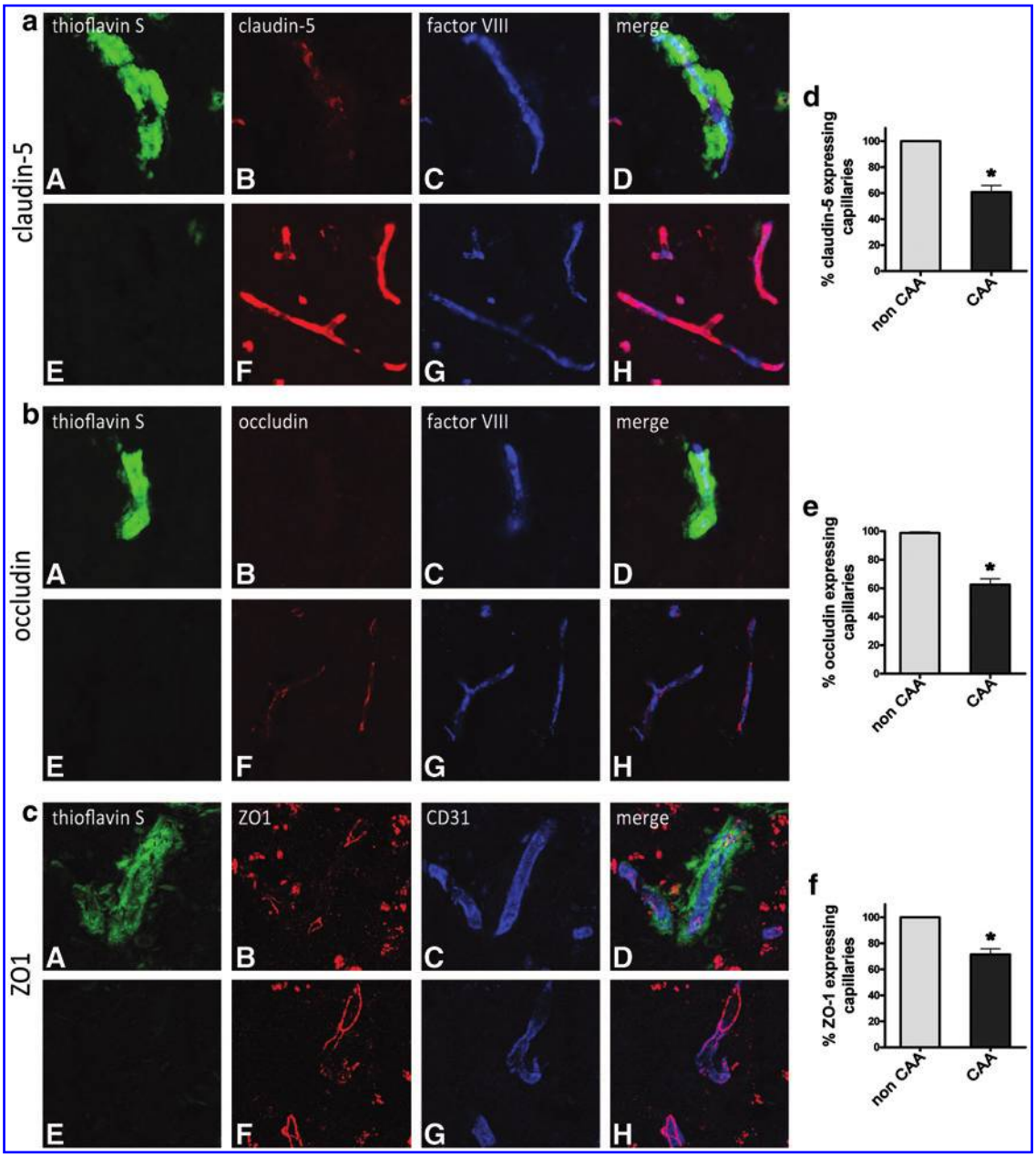

FIG. 2. Loss of TJ proteins in capCAA: co-localization study. Triple immunofluorescence analysis confirmed loss of TJs in endothelial cells affected by Aβ deposition; **(a)**, **(b)**, and **(c)** represent respectively analysis for TJ proteins claudin-5, occludin, and ZO1. Aβ was detected by Thioflavin S (*green*). Claudin-5, occludin, and ZO1 (*red*) were downregulated in capillaries detected by endothelial markers factor VIII and CD31 (*blue*). **(A, B, C, D)** Aβ-laden capillaries; **(E, F, G, H)** normal capillaries. Quantification of claudin-5 **(d)**, occludin **(e)**, and ZO-1 **(f)** expressing capillaries in CAA and non-CAA microvasculature is shown in the graphs. *$p < 0.05$, by Student *t* test (To see this illustration in color the reader is referred to the web version of this article at www.liebertonline.com/ars).

normal vascular expression pattern of TJ proteins in control tissue capillaries and in vessels not affected by Aβ deposition in samples from capCAA patients (Figs.1A, 1C, and 1E). Interestingly, we observed a marked reduction or even complete loss of occludin, claudin-5 and ZO-1 staining in CAA-affected capillaries (Figs.1B, 1D, and 1F). Quantification based on triple fluorescent staining for Aβ, TJs and an endothelium marker confirmed significant loss of TJ proteins expression in Aβ-laden capillaries compared to nonaffected capillaries (Figs. 2d–2f).

Aβ-laden capillaries are surrounded by NOX-2-positive activated microglia

Aβ is known to induce ROS-generating enzymes, including NOX-2 in microglia. NOX-2 is constitutively expressed by microglial cells and under physiological conditions NOX-2 activity is low. However, NOX-2 is strikingly upregulated in response to acute and chronic stimuli, including Aβ (24, 29). We show that NOX-2 is expressed in microglial cells in control brain tissue (Fig. 3A), however NOX-2 is abundantly and widely expressed in microglia throughout capCAA-affected tissue. Cells stained positive for NOX-2 were recognized as microglia based on their morphology (*e.g.*, characteristic long branching processes and a small cellular body). Particularly, Aβ-positive capillaries are engulfed by NOX2-immunoreactive microglia (Fig. 3B), strongly suggesting increased ROS production in close vicinity of Aβ-laden capillaries with TJ changes.

Aβ induces occludin and ZO-1 mRNA downregulation

Immunohistopathological findings showed reduced TJ expression in Aβ-laden capillaries. To investigate the direct effects of Aβ on mRNA expression of TJ proteins, we examined the effects of Aβ1-42 on occludin, claudin-5, and ZO-1, using a human cerebral microvascular endothelial cell line (hCMEC/D3) (44). Endothelial cells treated for 24 h with increasing concentration of Aβ fibrils (Fig. 4C)showed a dose-dependent significant reduction of occludin and ZO-1 transcripts (max reduction of 55% and 45%, respectively) (Figs. 4A and 4B). Remarkably, no changes in claudin-5 mRNA were detected (data not shown). These results are in line with the loss of occludin and ZO-1 in capCAA tissue, and suggest that reduced TJ protein expression might be caused by Aβ deposits in the microvasculature.

Aβ is toxic to brain endothelial cells via enhanced ROS production

In order to test which concentration of Aβ is lethal to brain endothelial cells, we performed a live/dead assay. Hereto, cells were incubated for 4 h and 24 h with different concentrations of Aβ1-42. Cells treated for 4 h with Aβ1-42 did not show any sign of cell death (data not shown), however after 24 h of Aβ treatment, we observed cell death using Aβ concentration of 10 μM and higher. No significant cytotoxicity was detected upon 1 μM Aβ treatment when compared to vehicle-treated cells (Fig .5A).

To evaluate the cytotoxic effect of Aβ on hCMECs, we assessed the effect on mitochondrial function as a measure of cell viability. We showed a dose-dependent decrease in brain endothelial cell viability after 24 and 48 h of Aβ1-42 treatment. After 24 h, a dose-dependent effect of Aβ on mitochondrial function was observed with a maximum effect at 1 μM Aβ1-42 with a decline of mitochondrial function around 50% (Fig .5B). Dose-dependent toxicity was also present at 48 h (data not shown).

We observed cell death and impaired mitochondrial function, which can both be related to ROS production (18, 38). In order to investigate whether Aβ1-42 induces production of ROS, hCMECs were treated with Aβ1-42 for 24 h. Using an Amplex Red assay, we showed that Aβ1-42 induced a dose-dependent increase in H_2O_2 production compared to vehicle-treated cells (Fig. 5C).

Antioxidants/ROS scavengers rescue endothelial cells from Aβ1-42 toxicity

Since we detected hydrogen peroxide production in response to Aβ incubation, we further elucidated the involve-

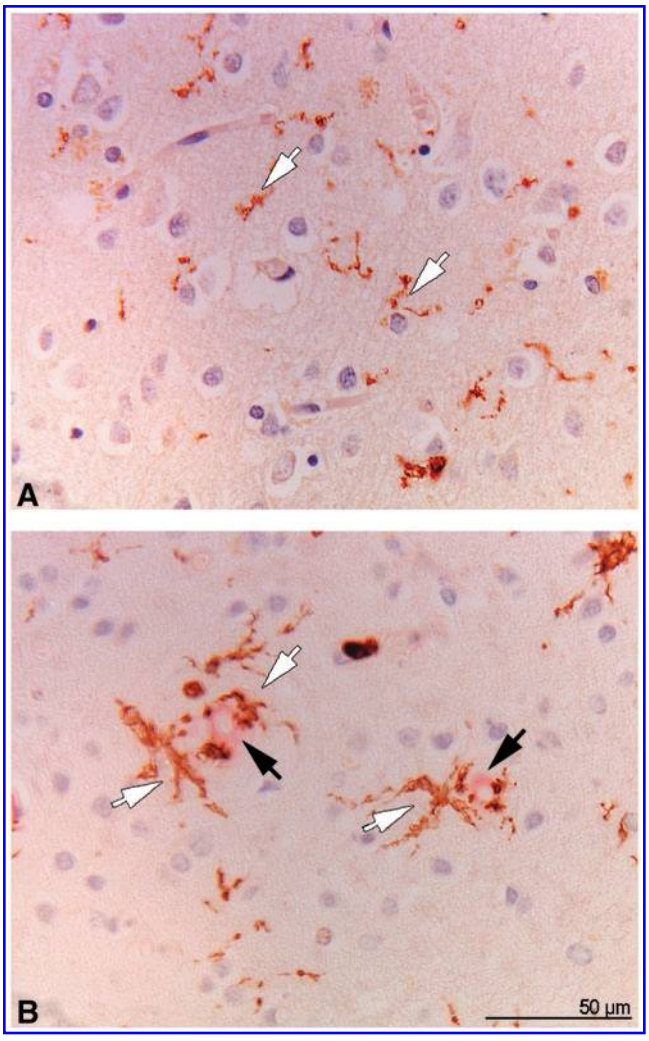

FIG. 3. NOX2 expression in capCAA. NOX2 is normally detected in microglia of control brains (**A**, *white arrows*). No immunoreactivity is detected in endothelial cells. In capCAA tissue, NOX2 immunoreactivity is increased in microglia (*white arrows*) and endothelial cells of Aβ-laden vasculature (*black arrows*) **(B)**. (To see this illustration in color the reader is referred to the web version of this article at www .liebertonline.com/ars).

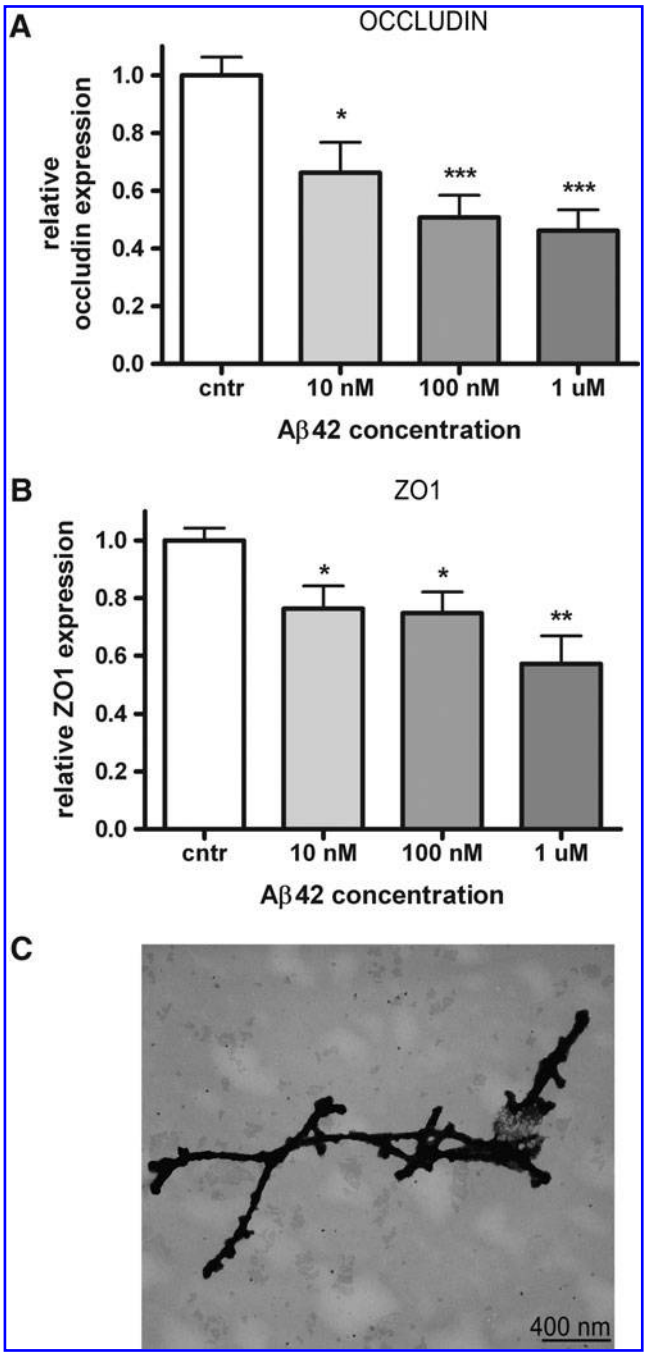

FIG. 4. Aβ induces downregulation of TJ proteins. Occludin **(A)** and ZO1 **(B)** mRNA expression was assessed by q-PCR on hCMEC upon 24 h Aβ treatment. Cells were treated with increasing concentration of Aβ1-42 (10 n*M*, 100 n*M*, 1 μ*M*). TJs expression was normalized to the expression of house-keeping gene GAPDH. Data were represented as the mean ± SEM; n = at least three experiments with triplicate samples. *$p < 0.05$, ***$p < 0.001$ by Student t test. Aβ fibrils were characterized by electron microscopy. **(C)** shows electron micrographs of Aβ1-42 incubated 3 days at 37°C prior to being added to the cell cultures.

ment of NADPH oxidase and xanthine oxidase in Aβ-mediated ROS production using specific inhibitors such as diphenylene iodonium (DPI) and allopurinol. Alpha-lipoic acid (alpha-LA) was used as general ROS scavenger. Endothelial cells preincubated with DPI, allopurinol, and alpha-LA for 2 h were then treated with different concentrations of Aβ1-42 (10 n*M* and 100 n*M*) in presence of the different compounds for 24 h. Cell viability was measured by MTT assay. DPI, allopurinol ,and LA were all able to rescue hCMECs from Aβ-mediated toxicity (Fig. 6), indicating that Aβ-mediated cytotoxicity is mainly due to Aβ-induced ROS production.

Antioxidants rescue Aβ-dependent downregulation of TJ proteins

We proved that Aβ1-42 fibrils induce ROS generation in our cell system and it has been previously shown that ROS can affect TJs integrity (34, 40). We hypothesized that the downregulation of TJ proteins observed upon Aβ1-42 fibrils treatment is due to the Aβ-dependent ROS production. To elucidate the link between Aβ, ROS, and TJs expression changes, we incubated hCMEC with allopurinol for 2 h prior to Aβ treatment; we then measured the expression of occludin and ZO-1 mRNA levels. As allopurinol was able to rescue cells from Aβ-mediated cytotoxicity, it was also capable of restoring TJ mRNA levels, confirming that indeed Aβ-driven ROS production is responsible for major TJ alterations (Fig. 7).

Upregulation of RAGE in capCAA

RAGE is the most important influx transporter for Aβ across the BBB and is expressed at relatively low levels in the microvasculature under physiological conditions. We show by means of immunohistochemical analysis a striking increase in RAGE expression in capCAA-affected capillaries compared to control and nonaffected capillaries. These results confirm, as previously reported (11), that Aβ induces a local upregulation of RAGE (Fig. 8).

RAGE mediates Aβ-induced cytotoxicity

In order to determine the involvement of RAGE in the Aβ cytotoxic effects, we treated hCMEC with a blocking antibody against RAGE. Cells were treated with the blocking antibody for 2 h and for 24 h together with Aβ1-42 fibrils. MTT assay showed that blocking RAGE rescued cells from Aβ-induced toxicity, demonstrating that Aβ effects on endothelial cells are exerted at least partially by its binding to RAGE (Fig. 9).

Discussion

For the first time, we show in this study a dramatic loss of TJ proteins in Aβ-laden capillaries, which are surrounded by NOX2-positive activated microglia. We demonstrated in an *in vitro* BBB system that Aβ is able to induce ROS formation and decrease TJ mRNA levels, which could be rescued upon pretreatment with NOX inhibitors and lipoic acid. We further demonstrate that blocking RAGE is a way to rescue cells from Aβ-induced toxicity.

Using our unique postmortem tissue, we here provide evidence on the loss of expression of TJ proteins in capCAA. So far, histopathological studies have demonstrated that microvascular alterations can be extensive in AD patients (8, 13).

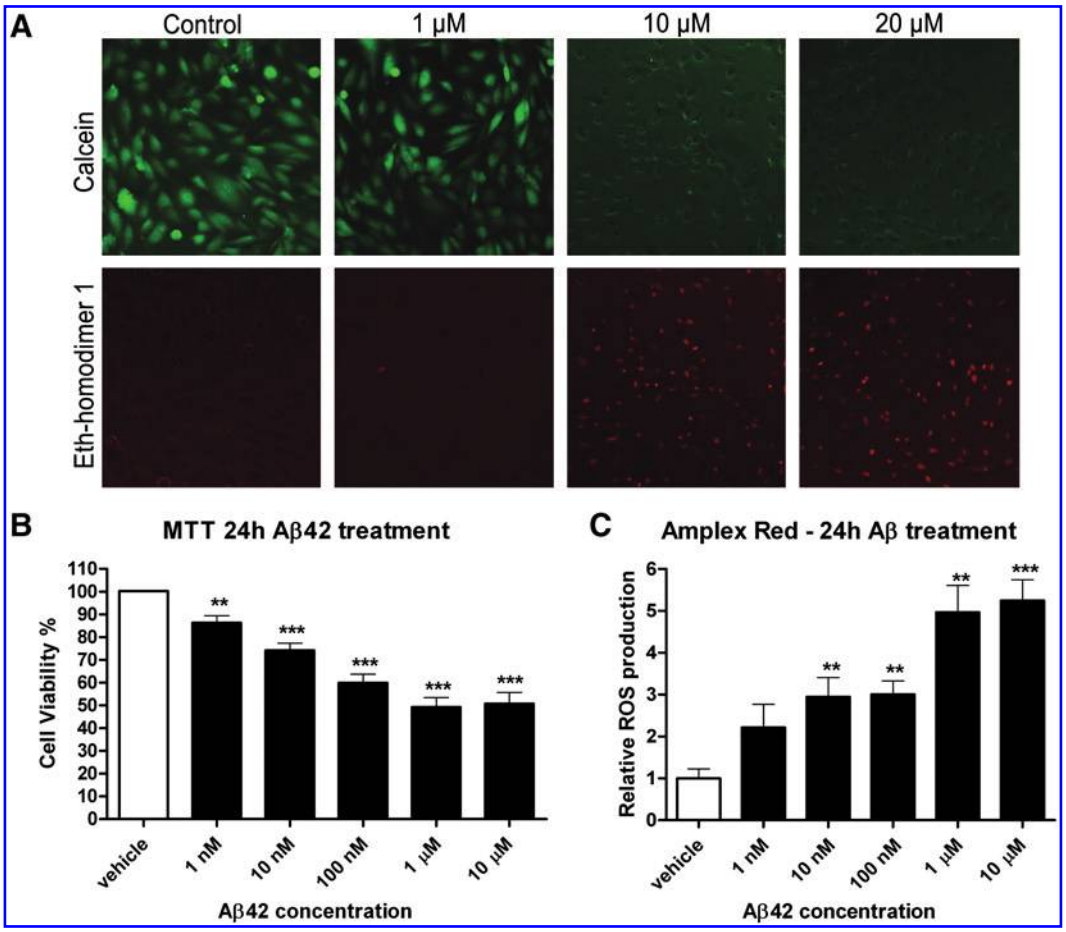

FIG. 5. Aβ cytoxicity and ROS production. HCMEC/D3 were incubated with increasing concentrations of Aβ1-42. Cells incubated for 24 h with 1 μM Aβ1-42 or less looked morphologically normal and appeared fluorescently *green* at the live/dead assay, no significant cells death was detected. At 10 μM or higher concentration, Aβ1-42 was toxic to hCMEC, dead *red* fluorescent cells were detected respect to control **(A)**. After 24 h incubation with Aβ42, there was a cell viability response in a dose-dependent manner with a maximum effect of 1 μM Aβ42 and a maximum decline of mitochondrial function around 50% measured by MTT assay **(B)**. The same treatment induced ROS production, here measured as production of H_2O_2. A dose-dependent H_2O_2 was observed after 24 h of treatment **(C)**. Data were represented as the mean ± SEM; n = at least three experiments with triplicate samples. $^{**}p < 0.01$, $^{***}p < 0.001$ by Student t test. (To see this illustration in color the reader is referred to the web version of this article at www.liebertonline.com/ars).

These alterations have been shown associated with vascular Aβ deposition as degeneration of perivascular cells, including pericytes and smooth muscle cells, swollen astrocytic end feet (17, 46), reduced expression of brain endothelial glucose transporter-1 protein, increased pinocytotic vesicles, and decreased numbers of mitochondria. In addition, prominent thickening and local disruption of vascular basement membranes was reported by several research groups analyzing either biopsy tissue or postmortem AD material (8, 26, 30). Vascular abnormalities that are associated with local amyloid accumulation suggest that impaired vascular function and thus impaired BBB integrity represents a common phenomenon in AD pathology. Although there are several studies demonstrating BBB alterations in CAA type II, comprehensive immunohistochemical studies on BBB abnormalities in Aβ-laden capillaries (CAA type I) are limited. *In vitro* studies support the idea that Aβ deposition affects BBB integrity since different Aβ peptides are able to increase endothelial permeability (6, 36) and induce altered expression and translocation of TJs proteins in human and animal ECs (15, 27). Remarkably, data on putative TJ alterations and the underlying mechanisms in CAA-affected capillaries are lacking.

To provide novel data on the BBB integrity during CAA, we selected a unique cohort of patients with abundant Aβ deposits in cortical capillaries. We observed a striking loss of occludin, claudin-5, and ZO-1 immunostaining in Aβ-laden capillaries, whereas unaffected capillaries showed a normal expression pattern, indicating that loss of TJ expression was predominantly related to microvascular Aβ deposition. Importantly, endothelial cells of capCAA-affected vessels still express endothelial markers, including factor VIII and CD31, excluding brain endothelial cell death as a potential reason for the lack of TJ protein expression. Although leakage of the BBB has been supported by elevated plasma proteins associated with Aβ deposits, we here for the first time provide direct evidence of TJ proteins loss in AD brains linked to Aβ accumulation. The subsequent breakdown of the BBB may in turn disrupt normal transport of nutrients, vitamins, and

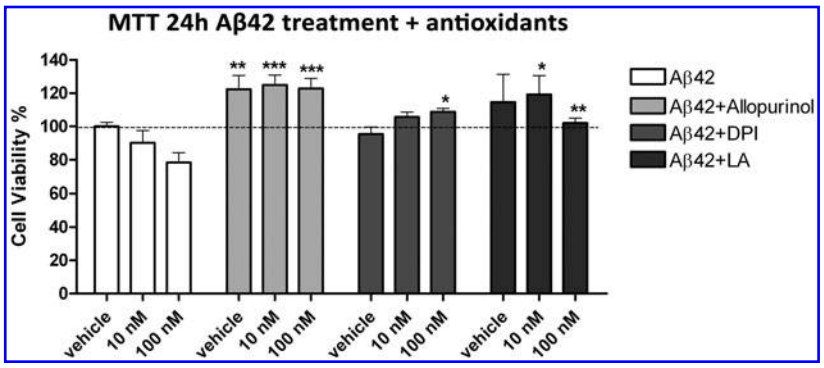

FIG. 6. Antioxidants rescue hCMEC from Aβ toxicity. HCMEC were preincubated for 2 h with antioxidants, allopurinol, DPI, and lipoic acid, before Aβ treatment. After preincubation, cells were treated with 10 n*M*, 100 n*M*, or vehicle in presence of the antioxidants. Antioxidants could reverse the toxic effect of Aβ1-42 on endothelial cells. Data were represented as the mean ± SEM; n = at least three. $^{*}p < 0.05$, $^{**}p < 0.01$, $^{***}p < 0.001$ by two-way ANOVA, followed by post hoc Bonferroni test.

electrolytes across the BBB, which are essential for proper neuronal functioning.

Interestingly, we detected enhanced expression of the ROS-generating enzyme NADPH oxidase-2 (NOX-2) in microglia surrounding Aβ-laden vessels. Previous data from our group demonstrated that deposition of Aβ throughout the brain parenchyma, especially extravascular deposition of Aβ that from the vessel wall radiates into the neuropil (named dyshoric changes), is able to induce an inflammatory response, consisting in activation of microglia and astrocytes (32, 33). Upon phagocytosis or recognition of Aβ by microglia cells, a series of responses may occur that includes the release of proinflammatory cytokines and ROS. One of the main sources of ROS under neuropathological conditions is enhanced NOX activity, together with the mitochondrial respiratory chain. In particular, NOX-2 is a well-known NADPH oxidase expressed in microglia where it is normally expressed at low levels. However, under pathological conditions, NOX-2 is upregulated and associated with a wide variety of vascular pathologies such as hypertension, diabetes, and hyperlipidemia (35). Enhanced expression of NOX-2 leads to increased ROS levels, particularly superoxide, and induces oxidative stress. In material derived from non-neurological controls, NOX-2 expression is mainly limited to microglia. Notably, the expression pattern of NOX-2 in capCAA tissue was strikingly different; revealing a stronger microglial expression, especially around capCAA-affected vessels, and NOX-2 was clearly expressed in perivascular macrophages associated with Aβ-laden capillaries. From these findings we conclude that Aβ deposition within and surrounding capillaries induces microglial activation and subsequent upregulation of NOX-2 protein expression in activated microglial cells and perivascular macrophages. These results support the idea of increased production of ROS in close proximity of capCAA-affected vessels and are in line with the observation that protein and DNA oxidative damage are increased in AD brains (25, 41).

To unravel pathways involved in BBB damage and Aβ-induced oxidative stress in brain endothelial cells, an *in vitro* approach was taken using the validated human brain endothelial cell line hCMEC/D3. We first assessed the cytotoxic effects of Aβ1-42, one of the predominant Aβ isoforms accumulating in Aβ-laden capillaries. Aβ1-40 is the predominant form of Aβ in larger CAA-affected vessels, such as arterioles and leptomeningeal vessels. However, the Aβ1-40/Aβ1-42 ratio of capillary Aβ is significantly lower than that of affected arteries and veins but equals that found in senile plaques (32), indicating that Aβ1-42 is a common Aβ isoforms in microvascular CAA. Furthermore, Aβ1-42 is known to be the most toxic form of Aβ to endothelial cells (12). Hence, we used the Aβ1-42 isoform for our *in vitro* studies. We treated endothelial cells with pre-aggregated Aβ peptide as aggregates were reported to be more toxic to ECs (5). At standardized conditions we could observe cells death after 24 h incubation at concentrations higher than 10 μM. Subtoxic concentrations of Aβ1-42 were then used to assess the effects of amyloid on TJ expression *in vitro*. Using this set-up, we showed a significant

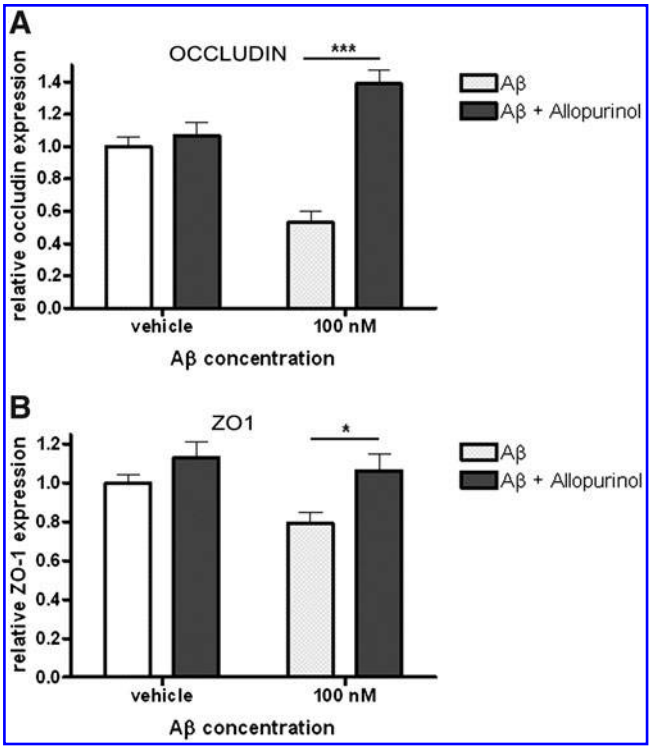

FIG. 7. Antioxidants rescue Aβ-dependent down-regulation of TJ proteins. Occludin **(A)** and ZO-1 **(B)** mRNA expression was assessed by q-PCR on hCMEC upon 24 h 100 μM Aβ treatment in the presence of allopurinol. TJs expression was normalized to the expression of house-keeping gene GAPDH. Co-treatment with allopurinol was able to restore normal levels of TJ transcripts. Data were represented as the mean ± SEM, n = at least three. $^{*}p < 0.05$, $^{***}p < 0.001$ by two-way ANOVA followed by post hoc Bonferroni test.

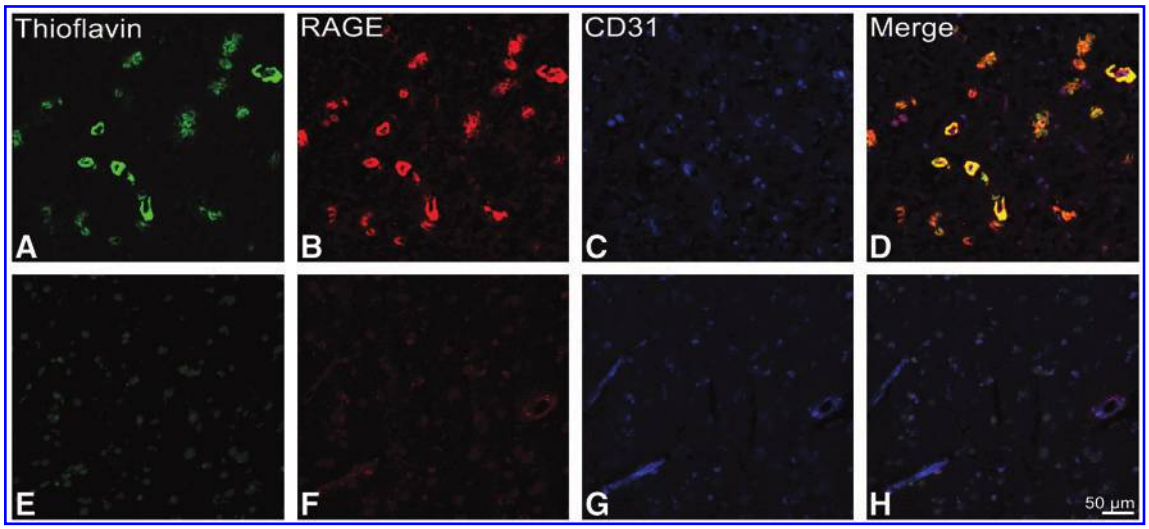

FIG. 8. RAGE expression in capCAA brain tissue. Expression of RAGE was detected by triple immunofluorescence analysis. Aβ was detected by Thioflavin S (*green*, **A** and **E**). No Aβ was detected in control tissue. RAGE (*red*) is strongly higher expressed in Aβ-laden capillaries **(B)** with respect to control **(F)**. Capillaries were stained with endothelial marker CD31 **(C, G)**. Merge show co-localization of Aβ and RAGE at capillary level in cap CAA **(D)**, but no co-localization in control tissue **(H)**. (To see this illustration in color the reader is referred to the web version of this article at www.liebertonline.com/ars).

dose-dependent downregulation of TJ proteins occludin and ZO-1 mRNA levels upon Aβ1-42 incubation, but no changes in claudin-5 mRNA level, as also reported by Tai *et al.* (36), which was in contrast to our postmortem findings. Reduced expression of occludin after 48 h of Aβ1-40 incubation has been previously described in hCMEC, but no changes in claudin-5 or ZO-1 (15). Aβ1-42 has been reported to reduce expression of claudin-5 and occludin in primary rat brain endothelial cells albeit at higher concentrations than the concentration used in this study (27). Our results, together with the previous findings, confirm the significant loss of occludin and ZO-1 in capCAA tissue and directly related these observations to Aβ deposit in the microvasculature. We speculate that claudin-5 protein expression may be altered by Aβ, as our immunohistochemical results strongly suggested. It is conceivable that prolonged exposure to Aβ is needed to decrease claudin-5 expression, as occurs in the patient material, or that loss of claudin-5 reported in capCAA tissue is not due to altered expression at transcriptional level but to a post-translational modification or degradation of the protein.

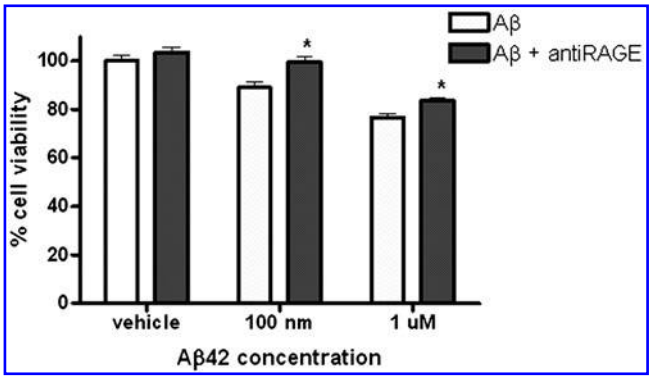

FIG. 9. Blocking RAGE rescue cell from Aβ cytotoxic effects. HCMEC were preincubated for 2 h with blocking antibody anti-RAGE (40 μg/ml) prior to Aβ1-42 treatment. Anti-RAGE was always present during treatment. Blocking RAGE could reverse the toxic effect of Aβ1-42 on endothelial cells. Data were represented as the mean ± SEM; n = at least three. *$p < 0.05$, by Student t test.

Our *in vitro* results showed dose-dependent decrease of mitochondrial function and increased production of ROS upon Aβ1-42 stimulation of hCMEC. One consequence of impaired mitochondrial function is enhanced generation of ROS, and since dysfunctional mitochondria will produce more ROS, a feed-forward loop is set up, resulting in a vicious cycle (42, 48). Aβ is also known to increase ROS production in different cerebral cell types and we showed that both NOX inhibition and exogenous antioxidants were able to counteract the toxic effect of Aβ1-42, confirming that reduced cell viability was indeed caused by ROS.

The cytotoxic effects of vascular Aβ might be caused by Aβ binding to RAGE. We observed for the first time a striking increase of RAGE expression in Aβ-laden capillaries. RAGE is a major influx transporter for Aβ across the BBB and its expression is upregulated in AD and transgenic models of amyloidosis in the affected cerebral vessels, microglia, and neurons (50). RAGE not only imports Aβ into the brain, increasing Aβ accumulation in the cerebral parenchyma, but when bound to its ligands also induces ROS production through NADPH oxidase activation (43). Importantly, we showed that blocking RAGE prevents Aβ-induced decrease of cell viability.

Conclusion

Taken together, we show the occurrence of severe TJ alterations in Aβ-laden capillaries. Interestingly, affected capillaries were surrounded by NOX2-positive activated microglia. *In vitro* experiments confirmed that Aβ was able to decrease TJ mRNA levels and that both exogenous

antioxidants as well as NOX inhibitors limit Aβ-mediated cellular toxicity. We further demonstrated that RAGE is the mediator of the Aβ-cytotoxic effects on endothelial cells. We speculate that due to increased local Aβ-driven ROS production, TJ protein expression is altered in the microvasculature of capCAA brains. It is plausible that extensive microvascular Aβ depositions, enhanced microvascular expression of RAGE, and concomitant loss of TJ protein expression impair BBB function and consequently leads to inefficient transport of nutrients into the brain. Collectively, these pathological processes might hamper Aβ clearance from the brain and thereby contribute to neuronal damage.

Acknowledgments

We thank N. Hahn (Department of Pathology, VU medical center, Amsterdam, the Netherlands) and Prof. Dr. D. Roos (Sanquin Research, Amsterdam, the Netherlands) for providing the NOX-2 antibody.

This work was financially supported by the 'Internationale Stichting Alzheimer Onderzoek' (ISAO grants 07517 and 09506) and the European Commission FP6 (ADIT, contract no. LSHB-CT-2005-511977).

Author Disclosure Statement

No competing financial interests exist.

References

1. Akiyama H, Ikeda K, Kondo H, and McGeer PL. Thrombin accumulation in brains of patients with Alzheimer's disease. *Neurosci Lett* 146: 152–154, 1992.
2. Attems J. Sporadic cerebral amyloid angiopathy: Pathology, clinical implications, and possible pathomechanisms. *Acta Neuropathol* 110: 345–359, 2005.
3. Attems J, Jellinger KA, and Lintner F. Alzheimer's disease pathology influences severity and topographical distribution of cerebral amyloid angiopathy. *Acta Neuropathol* 110: 222–231, 2005.
4. Babior BM. The NADPH oxidase of endothelial cells. *IUBMB Life* 50: 267–269, 2000.
5. Balcells M, Wallins JS, and Edelman ER. Amyloid beta toxicity dependent upon endothelial cell state. *Neurosci Lett* 441: 319–322, 2008.
6. Blanc EM, Toborek M, Mark RJ, Hennig B, and Mattson MP. Amyloid beta-peptide induces cell monolayer albumin permeability, impairs glucose transport, and induces apoptosis in vascular endothelial cells. *J Neurochem* 68: 1870–1881, 1997.

6a. Blasig IE, Bellmann C, Cording J, del Vecchio G, Zwanziger D, Huber O, and Haseloff RF. Occludin protein family: oxidative stress and reducing conditions. *Antioxid Redox Signal* 15: 1195–1219, 2011.

7. Braak H and Braak E. Neuropathological staging of Alzheimer-related changes. *Acta Neuropathol* 82: 239–259, 1991.
8. Claudio L. Ultrastructural features of the blood–brain barrier in biopsy tissue from Alzheimer's disease patients. *Acta Neuropathol* 91: 6–14, 1996.
9. Coisne C and Engelhardt B. Tight junctions in brain barriers during CNS inflammation. *Antioxid Redox Signal* 15: 1285–1303, 2011.
10. Deane R and Zlokovic BV. Role of the blood–brain barrier in the pathogenesis of Alzheimer's disease. *Curr Alzheimer Res* 4: 191–197, 2007.
11. Donahue JE, Flaherty SL, Johanson CE, Duncan JA, 3rd, Silverberg GD, Miller MC, Tavares R, Yang W, Wu Q, Sabo E, Hovanesian V, and Stopa EG. RAGE, LRP-1, and amyloid-beta protein in Alzheimer's disease. *Acta Neuropathol* 112: 405–415, 2006.
12. Eisenhauer PB, Johnson RJ, Wells JM, Davies TA, and Fine RE. Toxicity of various amyloid beta peptide species in cultured human blood–brain barrier endothelial cells: increased toxicity of dutch-type mutant. *J Neurosci Res* 60: 804–810, 2000.
13. Farkas E and Luiten PG. Cerebral microvascular pathology in aging and Alzheimer's disease. *Prog Neurobiol* 64: 575–611, 2001.
14. González-Mariscal L, Quirós M, and Díaz-Coránguez M. ZO proteins and redox-dependent processes. *Antioxid Redox Signal* 15: 1235–1253, 2011.
15. Gonzalez–Velasquez FJ, Kotarek JA, and Moss MA. Soluble aggregates of the amyloid-beta protein selectively stimulate permeability in human brain microvascular endothelial monolayers. *J Neurochem* 107: 466–477, 2008.
16. Hawkins BT and Davis TP. The blood–brain barrier/neurovascular unit in health and disease. *Pharmacol Rev* 57: 173–185, 2005.
17. Higuchi Y, Miyakawa T, Shimoji A, and Katsuragi S. Ultrastructural changes of blood vessels in the cerebral cortex in Alzheimer's disease. *Jpn J Psychiatry Neurol* 41: 283–290, 1987.
18. Hsu MJ, Sheu JR, Lin CH, Shen MY, and Hsu CY. Mitochondrial mechanisms in amyloid beta peptide-induced cerebrovascular degeneration. *Biochim Biophys Acta* 1800: 290–206, 2010.
19. This reference has been deleted.
20. Jeynes B and Provias J. The possible role of capillary cerebral amyloid angiopathy in Alzheimer lesion development: A regional comparison. *Acta Neuropathol* 112: 417–427, 2006.
21. Kalaria RN. The blood–brain barrier and cerebral microcirculation in Alzheimer disease. *Cerebrovasc Brain Metab Rev* 4: 226–260, 1992.
22. Lehner C, Gehwolf R, Tempfer H, Krizbai I, Hennig B, Bauer HC, and Bauer H. Oxidative stress and blood–brain barrier dysfunction under particular consideration of matrix metalloproteinases. *Antioxid Redox Signal* 15: 1305–1323, 2011.
23. Li G, Ma R, Huang C, Tang Q, Fu Q, Liu H, Hu B, and Xiang J. Protective effect of erythropoietin on beta-amyloid-induced PC12 cell death through antioxidant mechanisms. *Neurosci Lett* 442: 143–147, 2008.
24. Li JM and Shah AM. ROS generation by nonphagocytic NADPH oxidase: Potential relevance in diabetic nephropathy. *J Am Soc Nephrol* 14: S221–S226, 2003.
25. Lyras L, Cairns NJ, Jenner A, Jenner P, and Halliwell B. An assessment of oxidative damage to proteins, lipids, and DNA in brain from patients with Alzheimer's disease. *J Neurochem* 68: 2061–2069, 1997.
26. Mancardi GL, Perdelli F, Rivano C, Leonardi A, and Bugiani O. Thickening of the basement membrane of cortical capillaries in Alzheimer's disease. *Acta Neuropathol* 49: 79–83, 1980.
27. Marco S and Skaper SD. Amyloid beta-peptide1-42 alters tight junction protein distribution and expression in brain microvessel endothelial cells. *Neurosci Lett* 401: 219–224, 2006.
28. Overgaard CE, Daugherty BL, Mitchell LA, and Koval M. Claudins: control of barrier function and regulation in response to oxidant stress. *Antioxid Redox Signal* 15: 1179–1193, 2011.
29. Park L, Anrather J, Zhou P, Frys K, Pitstick R, Younkin S, Carlson GA, and Iadecola C. NADPH-oxidase-derived

reactive oxygen species mediate the cerebrovascular dysfunction induced by the amyloid beta peptide. *J Neurosci* 25: 1769–1177, 2005.
30. Perlmutter LS and Chui HC. Microangiopathy, the vascular basement membrane and Alzheimer's disease: A review. *Brain Res Bull* 24: 677–686, 1990.
31. Rensink AA, de Waal RM, Kremer B, and Verbeek MM. Pathogenesis of cerebral amyloid angiopathy. *Brain Res Brain Res Rev* 43: 207–223, 2003.
32. Richard E, Carrano A, Hoozemans JJ, van Horssen J, van Haastert ES, Eurelings LS, de Vries HE, Thal DR, Eikelenboom P, van Gool WA, and Rozemuller AJ. Characteristics of dyshoric capillary cerebral amyloid angiopathy. *J Neuropathol Exp Neurol* 69: 1158–1167, 2010.
33. Rozemuller JM, Eikelenboom P, Stam FC, Beyreuther K, and Masters CL. A4 protein in Alzheimer's disease: Primary and secondary cellular events in extracellular amyloid deposition. *J Neuropathol Exp Neurol* 48: 674–691, 1989.
34. Schreibelt G, Kooij G, Reijerkerk A, van Doorn R, Gringhuis SI, van der Pol S, Weksler BB, Romero IA, Couraud PO, Piontek J, Blasig IE, Dijkstra CD, Ronken E, and de Vries HE. Reactive oxygen species alter brain endothelial tight junction dynamics via RhoA, PI3 kinase, and PKB signaling. *FASEB J* 21: 3666–3676, 2007.
35. Sorce S and Krause KH. NOX enzymes in the central nervous system: From signaling to disease. *Antioxid Redox Signal* 11: 2481–2504, 2009.
36. Tai LM, Holloway KA, Male DK, Loughlin AJ, and Romero IA. Amyloid-beta-induced occludin down-regulation and increased permeability in human brain endothelial cells is mediated by MAPK activation. *J Cell Mol Med* 14: 1101–1112, 2010.
37. Thal DR, Ghebremedhin E, Rub U, Yamaguchi H, Del Tredici K, and Braak H. Two types of sporadic cerebral amyloid angiopathy. *J Neuropathol Exp Neurol* 61: 282–293, 2002.
38. Turrens JF. Mitochondrial formation of reactive oxygen species. *J Physiol* 552: 335–344, 2003.
39. van Horssen J, de Jong D, de Waal RM, Maass C, Otte–Holler I, Kremer B, Verbeek MM, and Wesseling P. Cerebral amyloid angiopathy with severe secondary vascular pathology: A histopathological study. *Dement Geriatr Cogn Disord* 20: 321–330, 2005.
40. van Wetering S, van Buul JD, Quik S, Mul FP, Anthony EC, ten Klooster JP, Collard JG, and Hordijk PL. Reactive oxygen species mediate Rac-induced loss of cell–cell adhesion in primary human endothelial cells. *J Cell Sci* 115: 1837–1846, 2002.
41. Wang J, Xiong S, Xie C, Markesbery WR, and Lovell MA. Increased oxidative damage in nuclear and mitochondrial DNA in Alzheimer's disease. *J Neurochem* 93: 953–962, 2005.
42. Wang X, Su B, Perry G, Smith MA, and Zhu X. Insights into amyloid-beta-induced mitochondrial dysfunction in Alzheimer disease. *Free Radic Biol Med* 43: 1569–1573, 2007.
43. Wautier MP, Chappey O, Corda S, Stern DM, Schmidt AM, and Wautier JL. Activation of NADPH oxidase by AGE links oxidant stress to altered gene expression via RAGE. *Am J Physiol Endocrinol Metab* 280: E685–694, 2001.
44. Weksler BB, Subileau EA, Perriere N, Charneau P, Holloway K, Leveque M, Tricoire–Leignel H, Nicotra A, Bourdoulous S, Turowski P, Male DK, Roux F, Greenwood J, Romero IA, and Couraud PO. Blood-brain barrier-specific properties of a human adult brain endothelial cell line. *FASEB J* 19: 1872–1874, 2005.
45. Wisniewski HM, Vorbrodt AW, and Wegiel J. Amyloid angiopathy and blood–brain barrier changes in Alzheimer's disease. *Ann NY Acad Sci* 826: 161–172, 1997.
46. Yamashita K, Miyakawa T, and Katsuragi S. Vascular changes in the brains with Alzheimer's disease. *Jpn J Psychiatry Neurol* 45: 79–84, 1991.
47. Zhou J, Zhang S, Zhao X, and Wei T. Melatonin impairs NADPH oxidase assembly and decreases superoxide anion production in microglia exposed to amyloid-beta1-42. *J Pineal Res* 45: 157–165, 2008.
48. Zhu X, Perry G, Moreira PI, Aliev G, Cash AD, Hirai K, and Smith MA. Mitochondrial abnormalities and oxidative imbalance in Alzheimer disease. *J Alzheimers Dis* 9: 147–153, 2006.
49. Zipser BD, Johanson CE, Gonzalez L, Berzin TM, Tavares R, Hulette CM, Vitek MP, Hovanesian V, and Stopa EG. Microvascular injury and blood–brain barrier leakage in Alzheimer's disease. *Neurobiol Aging* 28: 977–986, 2007.
50. Zlokovic BV. The blood–brain barrier in health and chronic neurodegenerative disorders. *Neuron* 57: 178–201, 2008.

Address correspondence to:
Anna Carrano
Department of Pathology, 1E23
VU University Medical Center
De Boelelaan 1117
1081 HV Amsterdam
The Netherlands

E-mail: a.carrano@vumc.nl

Date of first submission to ARS Central, January 30, 2011; date of acceptance, February 5, 2011.

Abbreviations Used

Aβ = amyloid β
AD = Alzheimer's disease
ARS = antigen retrieval step
BBB = blood–brain barrier
CAA = cerebral amyloid angiopathy
capCAA = capillary cerebral amyloid angiopathy
CERAD = Consortium to establish a Registry for Alzheimer's Disease
CNS = central nervous system
DAB = diaminobenzidine
DPI = diphenylene iodonium
ECs = endothelial cells
FBS = fetal bovine serum
HCMEC = human cerebral microvascular endothelial cell
HRP = horseradish peroxidase
LA = lipoic acid
MTT = 3-(4,5-dimethylthiazol-2-yl)-2,5-diphenyltetrazolium bromide
NF-κB = nuclear factor kappa-light-chain-enhancer of activated B cells
NOX = NADPH oxidase
O/N = overnight
PMD = postmortem delay
RAGE = receptor for advance glycation end products
ROS = reactive oxygen species
TJ = tight junction
ZO = zona occludens

This article has been cited by:

1. Lea Tenenholz Grinberg, Amos D. Korczyn, Helmut Heinsen. 2012. Cerebral amyloid angiopathy impact on endothelium. *Experimental Gerontology* . [CrossRef]
2. S Schiavone, V Jaquet, S Sorce, M Dubois-Dauphin, M Hultqvist, L Bäckdahl, R Holmdahl, M Colaianna, V Cuomo, L Trabace, K-H Krause. 2012. NADPH oxidase elevations in pyramidal neurons drive psychosocial stress-induced neuropathology. *Translational Psychiatry* **2**:5, e111. [CrossRef]
3. Benjamin S. Harvey, Katharina S. Ohlsson, Jesper L.V. Mååg, Ian F. Musgrave, Scott D. Smid. 2012. Contrasting protective effects of cannabinoids against oxidative stress and amyloid-# evoked neurotoxicity in vitro. *NeuroToxicology* . [CrossRef]
4. Anna Carrano, Jeroen J.M. Hoozemans, Saskia M. van der Vies, Jack van Horssen, Helga E. de Vries, Annemieke J.M. Rozemuller. 2012. Neuroinflammation and Blood-Brain Barrier Changes in Capillary Amyloid Angiopathy. *Neurodegenerative Diseases* **10**:1-4, 329-331. [CrossRef]
5. Linnea R. Freeman, Jeffrey N. Keller. 2011. Oxidative stress and cerebral endothelial cells: Regulation of the blood–brain-barrier and antioxidant based interventions. *Biochimica et Biophysica Acta (BBA) - Molecular Basis of Disease* . [CrossRef]
6. Fabien Gosselet, Pietra Candela, Roméo Cecchelli, Laurence Fenart. 2011. La barrière hémato-encéphalique. *médecine/sciences* **27**:11, 987-992. [CrossRef]
7. Erik Storkebaum, Annelies Quaegebeur, Miikka Vikkula, Peter Carmeliet. 2011. Cerebrovascular disorders: molecular insights and therapeutic opportunities. *Nature Neuroscience* **14**:11, 1390-1397. [CrossRef]
8. Zhiyou Cai, Bin Zhao, Anna Ratka. 2011. Oxidative Stress and #-Amyloid Protein in Alzheimer's Disease. *NeuroMolecular Medicine* . [CrossRef]
9. Lorenza González-Mariscal , Miguel Quirós , Monica Díaz-Coránguez . ZO Proteins and Redox-Dependent Processes. *Antioxidants & Redox Signaling*, ahead of print. [Abstract] [Full Text HTML] [Full Text PDF] [Full Text PDF with Links]
10. Ingolf E. Blasig , Reiner F. Haseloff . Tight Junctions and Tissue Barriers. *Antioxidants & Redox Signaling*, ahead of print. [Abstract] [Full Text HTML] [Full Text PDF] [Full Text PDF with Links]
11. Christian E. Overgaard , Brandy L. Daugherty , Leslie A. Mitchell , Michael Koval . Claudins: Control of Barrier Function and Regulation in Response to Oxidant Stress. *Antioxidants & Redox Signaling*, ahead of print. [Abstract] [Full Text HTML] [Full Text PDF] [Full Text PDF with Links]
12. Ingolf E. Blasig , Christian Bellmann , Jimmi Cording , Giovanna del Vecchio , Denise Zwanziger , Otmar Huber , Reiner F. Haseloff . Occludin Protein Family: Oxidative Stress and Reducing Conditions. *Antioxidants & Redox Signaling*, ahead of print. [Abstract] [Full Text HTML] [Full Text PDF] [Full Text PDF with Links]
13. Gianfranco Bazzoni . Pathobiology of Junctional Adhesion Molecules. *Antioxidants & Redox Signaling*, ahead of print. [Abstract] [Full Text HTML] [Full Text PDF] [Full Text PDF with Links]